



Petrography and Biostratigraphic Studies of Campano-Maastrichtian Sequences of Anambra Basin Southeastern Nigeria

J. O. Ayorinde^{1*}, O. C. Adeigbe² and Salufu Emmanuel³

¹*Department of Geology and Mineral Science, University of Ilorin, Ilorin, Nigeria.*

²*Department of Geology, University of Ibadan, Ibadan, Nigeria.*

³*Department of Geology, Federal Polytechnic Ede, Nigeria.*

Authors' contributions

This work was carried out in collaboration between all authors. Author JOA designed the study, went to the field with authors SE, JOA wrote the protocol and wrote the first draft of the manuscript. Author OCA supervised all the analyses of the study. All authors read and approved the final manuscript.

Article Information

DOI: 10.9734/CJAST/2018/39413

Editor(s):

(1) Aleksey Aleksandrovich Hlopitskiy, Professor, Department of Technology Inorganic Substances, Ukrainian State University of Chemical Technology, Ukraine.

Reviewers:

(1) José Martínez Reyes, University of the Ciénega of Michoacán State, México.

(2) Frederick Kelechi Onu, Nnamdi Azikiwe University Awka, Nigeria.

(3) Okon Emmanuel Etim, University of Calabar, Nigeria.

Complete Peer review History: <http://www.sciencedomain.org/review-history/24473>

Original Research Article

Received 16th January 2018

Accepted 6th April 2018

Published 5th May 2018

ABSTRACT

Anambra Basin located in the South Benue Trough is a Post Santonian synclinal sedimentary fill containing over 5000 m thick of Upper Cretaceous to Recent sediment. The study involved the use of field observation, sedimentological, petrographical and biostratigraphic studies of the sandstones and shale exposed within the study area to establish the depositional environment, textural and compositional maturity, provenance, tectonic settings, age relationship and to understand the stratigraphy of the basin. For this purpose, a total of 13 samples were subjected to heavy mineral and granulometric analyses, 9 samples of were subjected to micropaleontological analysis, and 2 samples of Ajali Sandstone were subjected to thin section analysis.

Field observations show that Enugu Shale is fissile with the presence of extraformational clast, Nkporo Group consists of shale, siltstone, mudstone and ironstone intercalation. Mamu Formation consists of shale, coal, and sandy shale unit, which graded into Ajali sandstone characterized by

*Corresponding author: E-mail: ayorinde.jo@unilorin.edu.ng;

cross beddings, herringbone structure and *ophiomorpha* burrows. The sieve analyses of the Ajali sandstone indicate that they are generally coarse grained, poorly to moderately sorted, mesokurtic to leptokurtic, nearly symmetrical to very coarse skewed. The result of bivariate analysis reveals that Ajali sandstone is fluvial sand, while the multivariate results show that some of the samples of Ajali Sandstone are shallow marine deposit while others are fluvial deposits. The textural result of Ajali Sandstone in the study area coupled with the field data such as Herringbone structures, and Ophiomorpha burrows, revealed that Ajali Sandstone was deposited in a tidal environment probably littoral environment. The paleocurrent direction of Ajali Sandstone measured from the beddings indicates southwest, while the provenance direction is toward the northeast. The Heavy mineral assemblages indicated from the heavy mineral analysis include: Zircon, Tourmaline, Rutile, Epidote, Garnet, Staurolite, Sillimanite, Chloritoid and Titanite which suggested their provenance to range from Acid igneous and Dynamothermal Metamorphic rock. The ZTR index indicates that the Sandstones were moderately mature mineralogically with a ZTR index that ranges from 11.54 to 58.3%. Thin section studies revealed the Sandstone to be quartz arenite to sublitharenite with more than 82% quartz. From the palynology and foraminiferal studies, it can be inferred that the paleo-environments of Nkporo, Enugu, and Mamu Shale were probably Marginal Marine environment based on the occurrence of forms such as *Phelodinium bolonienae*, Microforaminiferal wall linings, a large number of *Botryococcus braunii*, and dominance of arenaceous foraminiferal species. The age of Enugu/Nkporo Shales were suggested to be Early-Late Maastrichtian, the age of Mamu Shales were suggested to be Early Maastrichtian, and based on the occurrence of palynomorphs such as *Dinogymnium undulosum*, *Phelodinium bolonienae* and *Botryococcus braunii*. Based on the occurrence of foraminiferal such as *Haplophragmoides excavate*, the age of Enugu shale was suggested to be Coniacian-Maastrichtian.

Keywords: Anambra; mamu; heavy mineral; foraminiferal; botryococcus; Ajali.

1. INTRODUCTION

The Anambra Basin is one of the major sedimentary basins of Nigeria. It is found in the South Eastern part of Nigeria and comprises of a nearly triangular shaped embayment covering about 40,000 sq Km with a total sedimentary thickness of about 5 km. It is filled with Cretaceous and Tertiary sediments. The stratigraphic history of the basin is characterized by the second sedimentary phase (Campanian – Eocene) in south-eastern depositional cycle [1, 2]. This sedimentary phase was initiated by the Santonian folding and uplift of the Abakaliki anticlinorium along the NE-SW axis, and the consequent dislocation of the depocenter into the Anambra Basin on the northwest and the Afikpo syncline on the southeast [1,2]. The resulting succession comprises the Nkporo Group, Mamu Formation, Ajali Sandstone, Nsukka Formation, Imo Formation and Ameki Group. The origin of Benue Trough has generated much debate within the last three decades especially in relation to plate tectonics. The origin of the Anambra Basin is intimately related to the development of the Benue Rift. The Benue Rift was installed as the failed arm of a trilete fracture (rift) system, during the breakup of the +Gondwana supercontinent and the opening up of the southern Atlantic and Indian Oceans in the

Jurassic [3,4,5,6,7,8]. Burke [5] proposed a triple junction theory for the origin of the trough. They likened it to a ridge- ridge- ridge (r-r-r) triple junction. The three arm of the triple junction is the South Atlantic, the Gulf of Guinea and the Benue Trough. So far the most appropriate model to explain the evolution of Anambra Basin is the aulacogen theory by Olade [8,9]. The model is believed to start from uprising plume causing doming of crust with magma chamber developing underneath due to radiogenic heating at the base of the lithosphere. The rising magma causes domal uplift and volcanic eruptions, leading to the formation of Abakaliki volcanic rocks. Doming also causes a rift system, which made an r-r-r triple junction at the Gulf of Guinea. The system consists of an abandoned arm of a three-armed radial rift system. The other two arms continued to spread during the break-up of Gondwana, as South America separated from Africa, Petters [10].

The stratigraphy of Anambra Basin has been discussed by several authors [11,12,13,14,15] The basin comprises of over 2,000m of Campanian-Maastrichtian sequence arising from cycles of transgression and regression. The stratigraphy history of the region is characterized by three sedimentary phases [1,2] during which

the axis of the sedimentary basin shifted. These three phases are:

- (a) The Abakaliki-Benue phase (Aptian-Santonian)
- (b) The Anambra- Basin phase (Campanian-Mid Eocene)
- (c) The Niger Delta phase (Late Eocene-Pliocene)

Early Researchers and oil companies have done several studies on the petroleum potential of Anambra Basin, but result shows that the source rock which is the Enugu Shales, Nkporo Shales, and Mamu Shales have not attained thermal maturity that can guarantee petroleum

accumulation which led to discouragement and shift of attention to elsewhere. Recent studies on this area by Adeigbe and Salufu, [16] discovered from their research that the shale unit of Mamu Formation is thermally mature. This present study was carried on Nkporo, Mamu, Ajali Formation in Anambra Basin (Fig. 1).It involved field mapping and laboratory analyses of collected samples with the aim of using sedimentological, petrographical and biostratigraphical approaches in the deduction of the depositional environment, provenance, paleotectonic setting, paleoclimatic setting, age, the textural and mineralogical maturity of some Campano-Maastrichtian sediments in Anambra Basin.

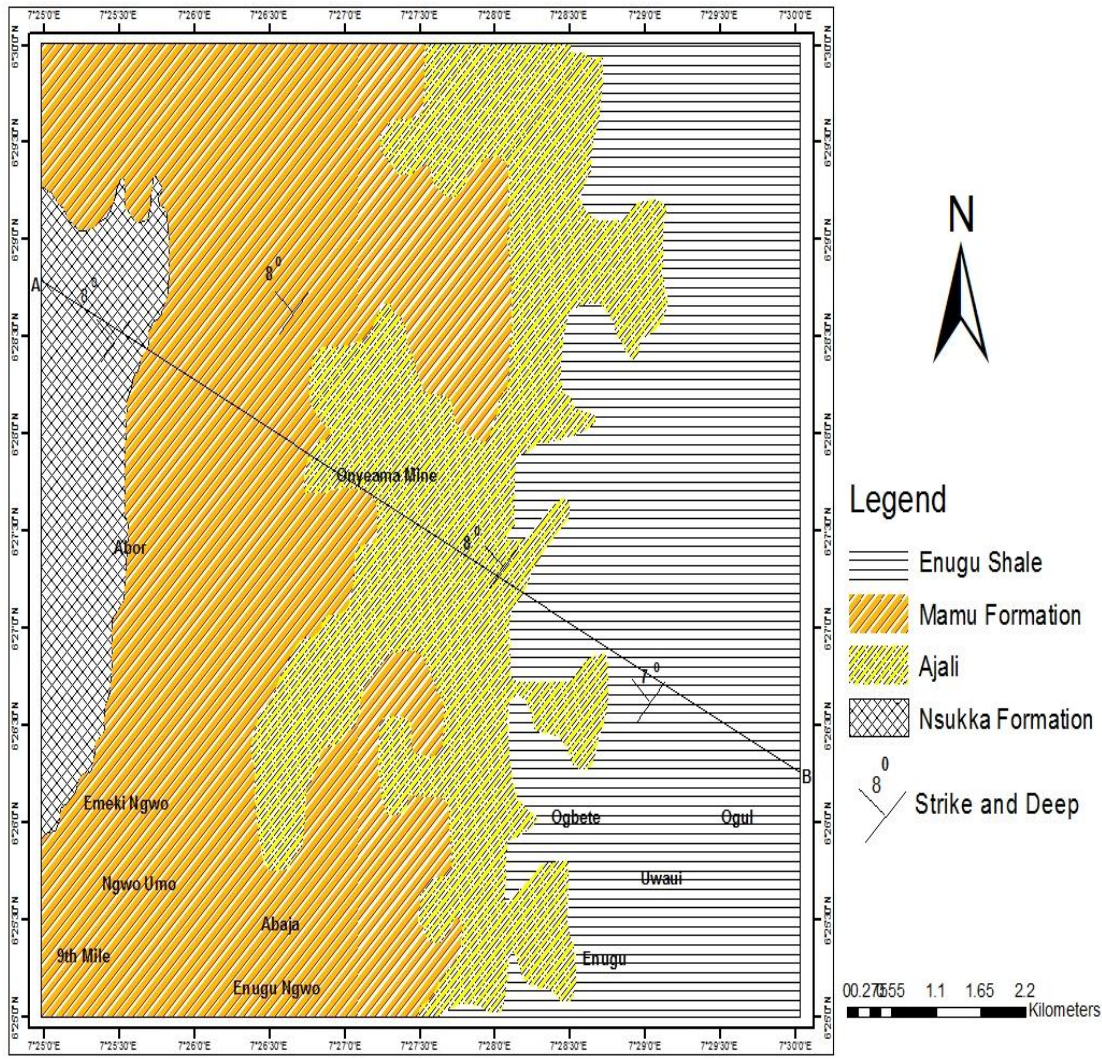


Fig. 1. Geology of the study area

2. METHODOLOGY

2.1 Field Mapping and Sampling

Geological field mapping started with a reconnaissance survey of the study area, followed by detailed field study and sampling, which covers the Enugu Shale, Nkporo Shale, Ajali Sandstone and Mamu Formations. A detailed study on the field includes mapping the geological structures such as beddings and layering, lithological description of the outcrop, biostratigraphic features and measurement such as dip and thickness of each bed.

13 samples were subjected to heavy mineral and sieve analysis, 9 samples of shale from Mamu, Nkporo and Enugu formation were subjected to micropaleontological analysis, and 2 samples were subjected to thin section analysis. The samples were collected from bottom to top of the formation.

2.2 Grain Size Analyses

Quantitative assessment of the percentages of different grain sizes in clastic sediments and sedimentary rocks is called granulometric analysis. Thirteen representative samples were collected from the study area. Ten of the samples were collected from Ajali Sandstone and the three other samples are mudstone and siltstone from Nkporo Group and siltstone from Mamu Formation. Samples that are weakly consolidated were disintegrated with a pestle and mortar. After disintegration, 100g of the sample is weighed and poured into a stacked sieve which has diameter of their aperture decreasing downwards. For this analysis eleven sieves were used and their phi scales are: -1.25, -0.25, 0.25, 0.75, 1.25, 1.75, 2.25, 2.75, 3.25, 3.75, >4.0. With these sieves clamped firmly in place, the sieve shaker was switched on and timed for 15 minutes. By weighing the contents of each sieve the distribution by weight of different size fractions can be determined. The weight of the grain retained in each sieves and pan were weighed, and the total of the weight of grain retained in each sieves is approximately equal to the weight of the sample poured at the beginning of the experiment. The weight retained, cumulative weight, cumulative weight percentage and individual weight percentage were calculated and tabulated in a table. The results from all these grain-size analyses are plotted on a statistical plot for each sample which includes histogram of the weight percentages of each of

the size fractions, a frequency curve, or a cumulative frequency curve.

2.3 Paleocurrent Analyses

The Dip and Azimuth of Twenty eight foreset of planar cross beds were measured from the cross-bedded unit of Ajali Sandstone exposed in the study area. The Measurement was carefully taken and recorded, from the measurement, the mean vector of the azimuths was calculated using the variable constraints system. The variance of the cross bedded units of the Ajali Sandstone was calculated following the method of Steinmetz [17] in order to determine the paleocurrent and depositional environment of Ajali Sandstone. A current rose diagram was constructed for the grouped data and this suggests the trend of the paleocurrent.

2.4 Heavy Mineral Analyses

Over 100 different heavy mineral is recorded from sediments, though they constitute not more than 0.1 to 0.5% of the clastic fraction, but they are very useful in provenance studies, transportation history, weathering characteristics and palaeogeography because of their stability [18]. Provenance studies in sandstones are often carried out by separating the heavy minerals from the bulk of the grains and identifying them individually. This procedure is called heavy mineral analysis and it can be an effective way of determining the source of the sediment. A total of 13 samples were selected for the heavy mineral analysis. 10 of which are sandstones from Ajali Formation, 1 siltstone and 1 mudstone from Nkporo Group and 1 siltstone from Mamu Formation. Each sample was sieved and the fraction retained by the 212 μ m mesh was preserved for used in the heavy mineral separation. The samples were then treated with dilute HCl for about two minutes to remove carbonates. Washing was done with distilled water to remove any acid and then the samples were dried on a hot plate. The gravity setting technique was employed for the separation of the heavy mineral. Heavy minerals are accessory mineral in sediment with a specific gravity greater than 2.85 which is the specific gravity of bromoform used to separate them from other light minerals such as feldspar and quartz. Apparatus and reagent employed include bromoform, acetone, dilute HCl, Canada balsam, filter paper, funnel and slides.

Dried samples are poured into a holding flask containing bromoform and the content was stirred vigorously until the heavy mineral could no longer be observed to settle into the stem of these separating funnel. The mixture was then allowed to settle for about 20 minutes, then the heavy mineral accumulated in the stem of the funnel was dropped into the filtering funnel by opening the stop lock carefully to drain the heavy minerals. The heavy mineral is then washed with acetone to remove the effect of acetone, allowed to dried and then mounted on glass slides with Canada balsam.

The heavy mineral was then viewed on the petrographic microscope to study their optical properties, shapes, size and number of different opaque and non-opaque mineral. The opaque mineral is studied using the reflected light while the non-opaque are studied using transmitted light. The dominant non-opaque mineral include zircon, rutile, and tourmaline, and this is used to calculate the maturity index or zircon-tourmaline-rutile (ZTR) index, using the Hubert formula as given below

$$\text{ZTR index} = \frac{\text{Zircon} + \text{Tourmaline} + \text{Rutile}}{\text{Total non-opaque mineral}} \times 100$$

2.5 Thin Section Analyses

Thin section of two semi-indurated sandstone was prepared in the laboratory. Each of the samples was mounted on a glass slide by Canada balsam and then heated on the hot plate. The mounted sample was then crushed on a lap wheel with a coarse abrasive and then washed in water. The slide was manually ground on a carborandum on a glass plate until the slide was thin enough for individual mineral identification. The slide was gently heated to remove bubbles and then allowed to dry before covering it with a slip and labeled in preparation for examination under a flat stage petrographic microscope. Based on these petrographic studies and using parameters such as grain shape, textural fabric and mineralogical composition, the textural and mineralogical maturity of the Sandstone can be revealed.

2.6 Palynological Analysis

The method of preparation follows the international standard of preparing palynological slides. The processes involve initial

decarbonisation using dilute hydrochloric acid; followed by sediment digestion through the use of Hydrofluoric acid (HF) soaked for 24hrs. The samples were later sieved with 5 μ nylon sieve in order to remove the clay sized particles. The samples were later subjected to maceral floatation by addition of heavy liquid such as Zn₂Br₄ in a centrifuge for 15 min at 2000 revolution/min. Suspended maceral was rinsed and mounted on glass slides with the aid of DPX mountant. The prepared palynological slides were observed under the scientific binocular microscope in order to analyze for palynological contents such as pollen, spores, dinoflagellates, fungal, algae and microforaminiferal wall lining. Point counts of the content were noted statistically while pictures of diagnostic forms were taken with Nikon digital camera. The preparation method was in accordance with standard methods [19,20,21].

2.7 Foraminiferal Sample Preparation Method

Weigh 20 g of each sample into each sample bowl, and the depth of samples are correctly transferred to clean aluminium sample bowls. 30ml of kerosene is poured into the sample and soaked overnight to disaggregate. Kerosene is drained out and the sample is then soaked in water. Diluted Hydrogen peroxide was added to the samples and left for about 15 minutes to soften the hard shale and free the microfossils. Each sample is then washed over a 63 microns sieve with water and detergent from a hand-directed water-jet. The residue collected from the sieve is replaced in the sample bowl and dried on the hot plate. The remaining residue is then sieved over 20 and 80 mesh sieves for the coarse and medium fractions while the finest residue in the receiver is treated as fine fraction. The coarse, medium and fine fractions are then stored in properly labeled sample phials for picking and analysis. This preparation method was in accordance with standard methods Green [22].

3. RESULTS AND INTERPRETATION

3.1 Field Description

Location 1: Road cut near fly-over along Enugu-Onitsha Expressway

Geological Unit: Enugu shale

Age: Campanian

Description: The outcrop is relatively extensive (Fig. 2) and highly weathered with a lateral extent of about 170 m and vertical extent of 17 m. The outcrop consists of shale, siltstone, heterolith and sandstone lithological unit. The shales are fined grained, dark grey in colour and highly fissile and they are often interbedded with siltstone and sandstones that may be ferruginised. The heterolith is the alternation of siltstone and shale;

they are brown in colour and contain extraformational clast (Fig. 3). The extraformational clast is spherical and well-rounded with a length of about 30cm. The siltstone usually occurs in lamina with sandstone unit intercalating each other. There is presence of normal fault which is assumed to be caused by dewatering and infiltration of water, gravitational unloading and offloading and soon.



Fig. 2. Engu shale exposed at a road cut near fly-over along Enugu-Onitsha expressway



Fig. 3. Extraformational clast in Engu shale at a road cut near fly over along Enugu-Onitsha expressway

Location 2: Agbogogu

Geological Unit: Nkporo Group

Age: Campanian

Description: The locality is extensive both laterally and vertically of about 100-120 m and 20-30m respectively. It consists of shale, siltstone, ironstone, mudstone and coal lithological unit with an average vertical thickness of 2 m. The shale unit consists of highly ferruginised shale, with shale- siltstone-mudstone heterolith with a thickness of about 8-10m. Ironstone is found in pockets along the bed just above the shale unit and it is hard and heavy. Following the ironstone is a coal bed of about 2-4m vertical thickness. It has a dull appearance with a dark grey colour, and it is highly weathered and disturbed with presence of rootlets of grasses.

Location 3: Below the bridge of Onyeama mine beside the Ekulu River

Geological unit: Mamu Formation

Age: Maastrichtian

Description: The outcrop is exposed laterally and vertically with about 50-70 m and 4-6m respectively. Four lithological unit were recognized as shale, coal, siltstone and heterolith. The basal unit of the outcrop is the heterolith which is the intercalation of sandstone

and siltstone, with a thickness of about 0.9-1.1 m. Overlying the heterolith is the dark grey carbonaceous shale unit which is fine grained and has a thickness of about 0.3-0.4 m, with a coal seam (Fig. 4) of about 0.8 m embedded within the overlying and underlying shale unit with a thickness of about 1.5 m. The whole sequence is covered by a fine to medium grained, the reddish brown bioturbated bed which have Ophiomorpha burrows with a thickness of about 1 m.

Location 4: Ngwo

Geological Unit: Ajali Sandstone

Age: Maastrichtian

Description: The outcrop is laterally and vertically extensive with thickness of about 100-150 m and 20-25 m respectively. The sandstone is light brown to reddish brown in colour (Fig. 5) and it is fined-medium grained in texture. The sandstone is friable, with rounded, sub-angular and moderately sorted grains, suggesting sediment maturity. The locality consists of 8 beds (Fig. 6) with an average thickness of about 3 m. Herringbone cross bedding is present on bed 5 and 6 indicating a high energy environment, Ophiomorpha burrows is observed on bed 4 and 7. Other structures include reactivation surface, wave ripple lamination and cross stratification. The bed dip to the S-E, S-W and N-E direction and the average dip amount is 8°.



Fig. 4. Coal seam at Onyeama bridge beside the Ekulu river

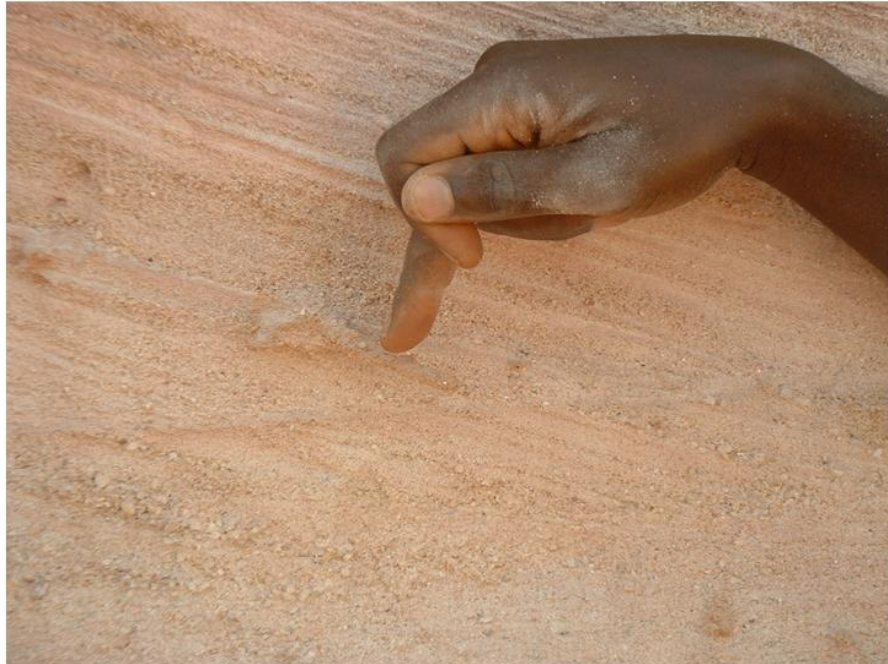


Fig. 5. Ajali Sandstone Showing cross bedding and Ophiomorpha burrow at Ngwo.

Location 5: Isimamu

Age: Maastrichtian

Geological unit: Ajali Sandstone

Description: The outcrop is very extensive laterally with a thickness of about 150-200metres. This outcrop consists of only sandstone unit which is white in colour and slightly indurated. It consists of two bed with an average thickness of 10feets. The texture varies from fine to medium grained sandstone.

$\tan^{-1} 1.8355$
 $= 61^{\circ}$
 Hence MVA = $61+180$
 $= 241^{\circ}$
 Variance = $\frac{\sum(A-MVA)^2}{N-1}$
 A=Azimuth
 MVA= Computed Vector Azimuth 241°
 N= Total No of outcome = 28
 Therefore variance = $48,080/(28-1)$
 $= 48080/27$
 $= 1,781$

3.2 Palaeocurrent Analysis

The result of the palaeocurrent analysis of the foreset of cross-bedded units of Ajali Sandstone (Table 1) shows that Ajali Sandstone has a mean vector azimuth of 241° which indicate the specific direction of provenance. Ajali Sandstone also has a variance of 1781 which indicate the variability of the provenance or flow direction. However, the rose diagram (Fig. 7) indicates paleocurrent direction towards southwest while provenance direction is towards the northeast direction (Fig. 7).

Mean Vector Azimuth = $\tan^{-1}(\sum \sin A) / (\sum \cos A)$

$\tan^{-1} (-18.8705) / (-10.2807)$

3.3 Granulometric Analyses

Graphic mean: Mean size is a function of the size range of the sand grains as well as the amount of energy imparted to the sediment which most times depends on the velocity of the transporting agent. The Graphic mean distribution for the samples collected from the study area ranges between 0.25ϕ - 1.37ϕ , with a mean value of 0.899 which indicate that the sediment is coarse grained sand. [23]. This also suggests that the samples were deposited in a high energy environment, which is an environment of high tidal or wave action, that favours the deposition of coarse grained sediment. The siltstone and mudstone of Nkporo and Mamu Formation are medium to coarse grain sand.

| FT | DEPTH(FT) | AGE | LITHOLOGY | LITHOLOGY DESCRIPTION |
|------|-----------|---------------|-----------------|---|
| 99.1 | 20 | MAASTRICHTIAN | AJALI SANDSTONE | Reddish brown sandstone facies with fine to medium grained sand particles. Presence of cross bedding, herringbone bedding and burrows. |
| 79.1 | 12.7 | MAASTRICHTIAN | MAMU FORMATION | About 4-6m thick of shale-siltstone heterolith with coal seams embedded within the shale unit. The shale unit is highly weathered because of the presence of stream flowing beside the outcrop. |
| 66.4 | 23.5 | CAMPANIAN | NKPORO GROUP | Highly ferruginised shale-siltstone-mudstone heterolith with presence of ironstone present in pockets in the shale unit. The coal unit has a dark gray colour with presence of rootlets of grasses. |
| 42.9 | 42.9 | CAMPANIAN | ENUGU FORMATION | Heterolith of shale-siltstone facies with presence of extraformational clast. Grey fissile shale unit |

Fig. 6. The composite local stratigraphy of the study area

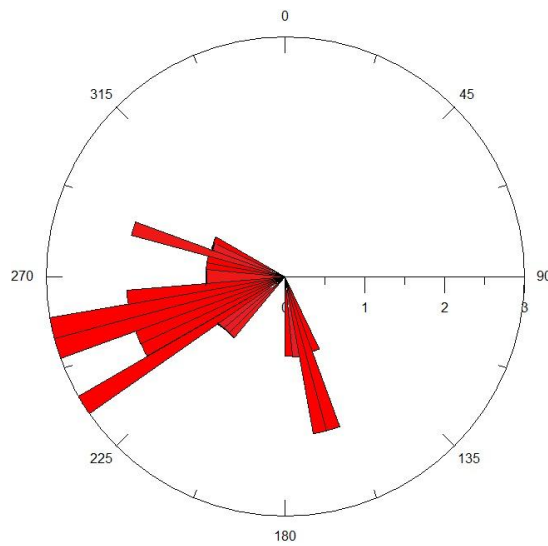


Fig. 7. Rose plot for ajali sandstone

Table 1. Paleocurrent analysis of ajali sandstone

| S/N | Azimuth (A) | Dip (D) | Sin A | Cos A | Cos D | b=CosA×D | A=SinA×D | (MVA--A) ² |
|-----|-------------|---------|----------|----------|--------|----------|----------|-----------------------|
| 1 | 260 | 18 | -0.9848 | -0.1736 | 0.9511 | -0.1651 | -0.9366 | 361 |
| 2 | 265 | 17 | -0.9962 | -0.0871 | 0.9563 | -0.0833 | -0.9527 | 576 |
| 3 | 257 | 18 | -0.9744 | -0.2250 | 0.9511 | -0.2140 | -0.9268 | 256 |
| 4 | 262 | 20 | -0.9903 | -0.1392 | 0.9397 | -0.1308 | -0.9306 | 441 |
| 5 | 255 | 16 | -0.9659 | -0.2588 | 0.9613 | -0.2488 | -0.9285 | 196 |
| 6 | 250 | 20 | -0.9396 | -0.3420 | 0.9397 | -0.3214 | -0.8829 | 81 |
| 7 | 290 | 25 | -0.9396 | 0.3420 | 0.9063 | 0.3099 | -0.8512 | 2401 |
| 8 | 300 | 22 | -0.8660 | 0.5000 | 0.9272 | 0.4636 | -0.8030 | 3481 |
| 9 | 285 | 25 | -0.9659 | 0.2588 | 0.9063 | 0.2346 | -0.8754 | 1936 |
| 10 | 165 | 24 | 0.2588 | -0.9659 | 0.9135 | -0.8823 | 0.2364 | 5776 |
| 11 | 170 | 25 | 0.1736 | -0.9848 | 0.9063 | -0.8925 | 0.1573 | 5041 |
| 12 | 170 | 22 | 0.1736 | -0.9848 | 0.9272 | -0.9131 | 0.1610 | 5041 |
| 13 | 162 | 20 | 0.3090 | -0.9511 | 0.9397 | -0.8937 | 0.2904 | 6241 |
| 14 | 290 | 18 | -0.9396 | 0.3420 | 0.9511 | 0.3253 | -0.8937 | 2401 |
| 15 | 280 | 24 | -0.9848 | 0.1736 | 0.9135 | 0.1586 | -0.8996 | 1521 |
| 16 | 156 | 22 | 0.4067 | -0.9135 | 0.9272 | -0.8470 | 0.3771 | 7225 |
| 17 | 178 | 24 | 0.0340 | -0.9993 | 0.9135 | -0.9129 | 0.0318 | 3969 |
| 18 | 225 | 20 | -0.7070 | -0.7070 | 0.9397 | -0.6644 | -0.6644 | 256 |
| 19 | 240 | 18 | -0.8660 | -0.5000 | 0.9511 | -0.4755 | -0.8237 | 1 |
| 20 | 242 | 18 | -0.8829 | -0.4695 | 0.9511 | -0.4465 | -0.8397 | 1 |
| 21 | 250 | 14 | -0.9396 | -0.3420 | 0.9703 | -0.3318 | -0.9167 | 81 |
| 22 | 230 | 14 | -0.7660 | -0.6428 | 0.9703 | -0.6237 | -0.7432 | 121 |
| 23 | 245 | 14 | -0.9063 | -0.4226 | 0.9703 | -0.4100 | -0.8794 | 16 |
| 24 | 238 | 20 | -0.8480 | -0.5299 | 0.9397 | -0.4979 | -0.7967 | 9 |
| 25 | 260 | 20 | -0.9848 | -0.1736 | 0.9397 | -0.1631 | -0.9254 | 361 |
| 26 | 254 | 18 | -0.9613 | -0.2756 | 0.9511 | -0.2621 | -0.9143 | 169 |
| 27 | 240 | 18 | -0.8860 | -0.5000 | 0.9511 | -0.4755 | -0.8237 | 1 |
| 28 | 252 | 14 | -0.9511 | -0.3090 | 0.9703 | -0.3000 | -0.9229 | 121 |
| | | | -18.8705 | -10.2807 | | | | 48080 |

Table 2. Group data of the rose diagram for Ajali Sandstone

| Class Interval | Tally | Frequency |
|----------------|-------------|-----------|
| 151-180 | IIII I | 6 |
| 181-210 | - | - |
| 211-240 | IIII | 5 |
| 241-270 | IIII IIII I | 12 |
| 271-300 | IIII | 5 |
| 301-330 | - | - |
| 331-360 | - | - |

3.4 Standard Deviation/Sorting

Sorting is the measure of standard deviation and it refers to the pattern of spread of grain size, which indicates the fluctuation in the kinetic energy (sorting) of the depositing medium. The result and description of analyzed samples indicate poorly sorted to moderately sorted (between 0.77Ø to 1.22Ø) with a mean of 0.956, and most of the samples falling in the moderately sorted. This means that the sediment was

deposited with a slight fluctuation in the kinetic energy of the transporting medium. The siltstone and mudstone of Nkporo and Mamu Formation are very poorly sorted, which reflects an increased fluctuation of energy conditions of the depositing medium and hence a very poor winnowing ability [23].

3.5 Skewness

Samples analyzed were discovered to be between near symmetrical to fine-skewed (-0.01Ø-0.14Ø), with most samples showing near symmetrical and others showing coarse-skewed. For the coarse skewed samples, it implies that the velocity of the depositing agent operated at a higher value than the average velocity for a greater length of time than normal. The coarse skewed sediment is typical of littoral or beach environment where the winnowing action of wave and tidal currents are dominant, while near symmetrical skewness reflects that broad spectrum of the population is present in the sample [23].

3.6 Kurtosis

Majority of the sandstone samples are leptokurtic with a few mesokurtic and platykurtic. However flat curves of poorly sorted sediment are platykurtic while the strongly peaked curve of good sorting is leptokurtic. These means that most of the sandstone samples are moderately to well sorted [23].

3.7 Multivariate Parameters

From the result and interpretation (Table 4), it can be suggested that Ajali sandstones were deposited in a shallow marine environment which was interfered by fluvial environment by the

shallowing upward regime of the basin. The result for the siltstone and mudstone of Nkporo and Mamu Formation shows that they were deposited in a fluvial environment after the method of Sahu [24].

In conclusion, it can be suggested that the grain size parameters used for analyzing these sandstone samples collected from the study area, all indicate that the sands are moderately sorted and that kinectic energy condition for deposition was predominantly high with much increased fluctuation in energy accounting for high energy condition and this can be confirmed with the cross bedding and herringbone structure that was identified in the formation.

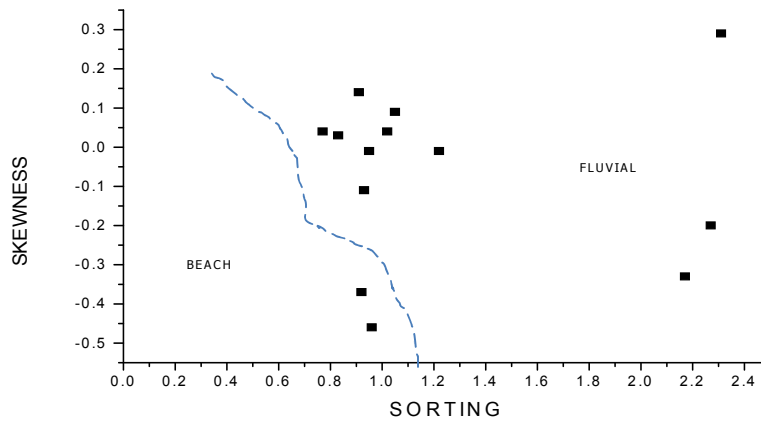


Fig. 8. Graph of skewness against sorting Friedman [25]

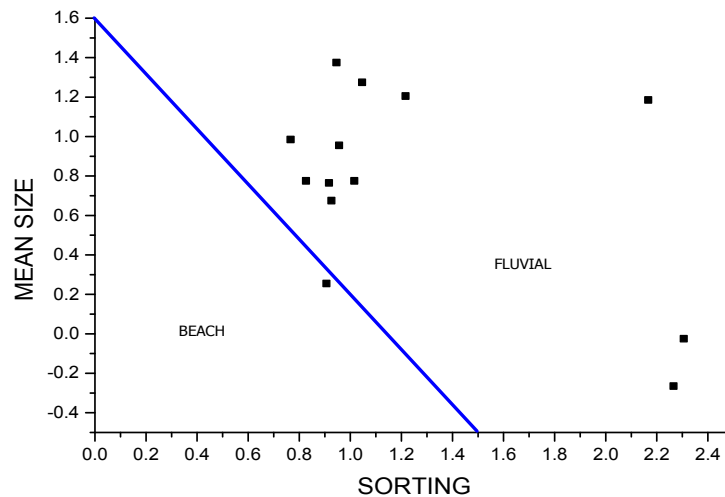


Fig. 9. Graph of mean size against sorting Moiola and Weiser [26]

Table 3. Computed result of the univariate parameter derived from probability plots of Ajali sandstone, Nkporo mudstone and Mamu siltstone

| Sample no | Sorting | Value | Skewness | Value | Mean size | Value | Kurtosis | Value |
|----------------------|--------------------|--------------|---------------------|--------------|------------------|--------------|------------------|--------------|
| B1 AJALI SANDSTONE | Moderately sorted | 0.96 | Very coarsed skewed | -0.46 | Coarse sand | 0.95 | Platykurtic | 0.67 |
| B2 AJALI SANDSTONE | Moderately sorted | 0.92 | Very coarsed skewed | -0.37 | Coarse sand | 0.76 | Leptokurtic | 1.33 |
| B3 AJALI SANDSTONE | Moderately sorted | 0.93 | coarsed skewed | -0.11 | Coarse sand | 0.67 | Mesokurtic | 1.07 |
| B4 AJALI SANDSTONE | Moderately sorted | 0.83 | Nearly symmetrical | 0.03 | Coarse sand | 0.77 | Leptokurtic | 1.17 |
| B5 AJALI SANDSTONE | Moderately sorted | 0.77 | Nearly symmetrical | 0.04 | Coarse sand | 0.98 | Leptokurtic | 1.11 |
| B6 AJALI SANDSTONE | Poorly sorted | 1.05 | Nearly symmetrical | 0.09 | Medium sand | 1.27 | Mesokurtic | 1.07 |
| B7 AJALI SANDSTONE | Poorly sorted | 1.02 | Nearly symmetrical | 0.04 | Coarse sand | 0.77 | Leptokurtic | 1.21 |
| B8 AJALI SANDSTONE | Moderately sorted | 0.95 | Nearly symmetrical | -0.01 | Medium sand | 1.37 | Leptokurtic | 1.18 |
| B9 AJALI SANDSTONE | Moderately sorted | 0.91 | Fine skewed | 0.14 | Coarse sand | 0.25 | Leptokurtic | 1.37 |
| B10 AJALI SANDSTONE | Poorly sorted | 1.22 | Nearly symmetrical | -0.01 | Medium sand | 1.2 | Mesokurtic | 1.05 |
| B11 NKPORO MUDSTONE | Very Poorly sorted | 2.31 | Very Fine skewed | 0.29 | Coarse sand | -0.03 | Very platykurtic | 0.26 |
| B12 NKPORO SILTSTONE | Very Poorly sorted | 2.27 | coarsed skewed | -0.20 | Coarse sand | -0.27 | Mesokurtic | 0.99 |
| B13 MAMU SILTSTONE | Very Poorly sorted | 2.17 | Very coarsed skewed | -0.33 | Medium sand | 1.18 | Mesokurtic | 1.03 |

Table 4. Multivariate result of the samples from the studied area (After Sahu, [24])

| Sample | Results | Interpretation |
|----------------------|-------------|----------------|
| B1 AJALI SANDSTONE | -5.855926 | Shallow marine |
| B2 AJALI SANDSTONE | -5.968272 | Shallow marine |
| B3 AJALI SANDSTONE | -7.3663085 | Shallow marine |
| B4 AJALI SANDSTONE | -7.1419715 | Shallow marine |
| B5 AJALI SANDSTONE | -6.6082765 | Shallow marine |
| B6 AJALI SANDSTONE | -9.2250825 | Fluvial |
| B7 AJALI SANDSTONE | -8.853461 | Fluvial |
| B8 AJALI SANDSTONE | -7.8258955 | Fluvial |
| B 9 AJALI SANDSTONE | -8.5197235 | Fluvial |
| B10 AJALI SANDSTONE | -10.245967 | Fluvial |
| B11 NKPORO MUDSTONE | -21.6516915 | Fluvial |
| B12 NKPORO SILTSTONE | -18.9368695 | Fluvial |
| B13 MAMU SILTSTONE | -17.0092385 | Fluvial |

3.8 Bivariate Parameter

From the bivariate plot of sorting against skewness (Fig. 8) and the plot of sorting against mean size (Fig. 9), it can be concluded that most of the sediment is fluvial sand.

3.9 Heavy Mineral Analysis

Heavy mineral has long been used as indices of provenance. Certain species are characteristic of certain source rocks. These heavy mineral were viewed and identified under the microscope by using the following diagnostic optical properties such as transparency, translucency, isotropism or anisotropism and extinction. Based on the above properties the following heavy minerals were identified under the microscope:

Zircon: Usually colorless to pale brown in thin section, although high relief and small grain size tend to make it look darker. In grain mount, the color may be more apparent with weak pleochroism, so that grains are darker when the long axis is aligned parallel to the vibration direction of the lower polar. Some samples may be cloudy due to numerous inclusions or may show concentric color zoning or patchy color. Commonly occurs as euhedral to subhedral tetragonal crystals with pyramidal terminations. Cleavages are poor and not usually seen in thin section. Not usually twinned, but twinning occurs occasionally.

Tourmaline: It appears as long slender to thick prismatic and columnar crystals, with a triangular shape in cross section. It is rarely perfectly euhedral and it has a moderately high birefringence, negative elongation and straight

extinction, with wide range of colour such as pink, brown, bluish green, green, or colourless.

Rutile: Appears as elongate to sub-round to sub-angular prismatic grains, which are often transparent or subtranslucent with a wide range of colour such as red, reddish brown, reddish black or almost opaque in thin section. Pleochroism is weak, may be color zoned. Good cleavage and twinning are common. Elongate sections show parallel extinction and the Birefringence is extreme.

Epidote: Pleochroic in shades of light pistachio green, moderately high birefringence, optically negative, with inclined extinction.

Chloritoid: Usually light to medium green in thin section and pleochroic, expressed in shades of colorless, pale green, yellowish green, green, or brownish green. Birefringence is usually low, one set of micaceous cleavage, inclined extinction, generally positive with moderate 2V, lamellar twinning common.

Garnet: Crystals rounded or equant with no birefringence, no pleochroism, No cleavage, often show irregular fractures, and no twinning.

Titanite: it can be determined from its "sphenoidalshape" as seen in a thin section Because titanite has a very high birefringence, it will appear as a high order white under crossed nicols. Titanite can also be recognized by its very high relief.

Sillimanite: Water clear, moderately high birefringence, low 2V, biaxial positive, elongation positive, prismatic grains with transverse cracks,

straight extinction. Often aggregates of very fine needle-like fibers.

Staurolite: In thin sections staurolite is commonly twinned and shows lower first order birefringence similar to quartz, with the twinning displaying optical continuity. Strongly pleochroic in shades of deep yellow and brownish yellow, birefringence low, extinction straight.

It was observed from the analysis (Table 3) that the non-opaque minerals like epidote, chloritoid, garnet, titanite, staurolite, predominate the other non-opaque mineral such as tourmaline, rutile, and zircon. Different mineral assemblages represent a certain source origin (Table 2). From this analysis, the mineral association (Table 4) suggests a provenance ranging from acid igneous rock to dynamothermal metamorphic rocks origin. From the plot (Fig. 2), it is seen that most of the sample falls on the rutile axis, which indicates the predominance of rutile.

3.10 Thin Section Petrography

From the recalculated framework composition of Quartz, feldspar, and rock fragment (Table 7), a

ternary diagram for the classification of the sandstone based on framework composition was constructed.[18]. Likewise, the result of petrographic analysis as shown in Table 7 ranges the Quartz percentage from 83% to 92%, and the Rock fragment percentage from 8% to 17%, with no feldspar content. This all indicates that the sandstone is an arenite (Fig. 12). Sample A is Quartz arenite (Fig. 12), and the shape of the quartz grain is angular to subangular, while the shape of the rock fragment is subangular to subrounded. Sample B is sub litharenite (Fig. 12), with the shape of the quartz grain been subangular to subrounded, while the rock fragment is subrounded to rounded. This indicates that sample A has not undergone a long transportation process before they were deposited and the energy of the transporting medium is not high to create abrasion that makes the grains rounded. The absence of feldspar in the sandstone also indicate that the sediment have undergone a long transportation history before deposition because all the feldspar have been weathered away as a result of humidity. Therefore the sandstone can be said to be compositionally matured and texturally immature.

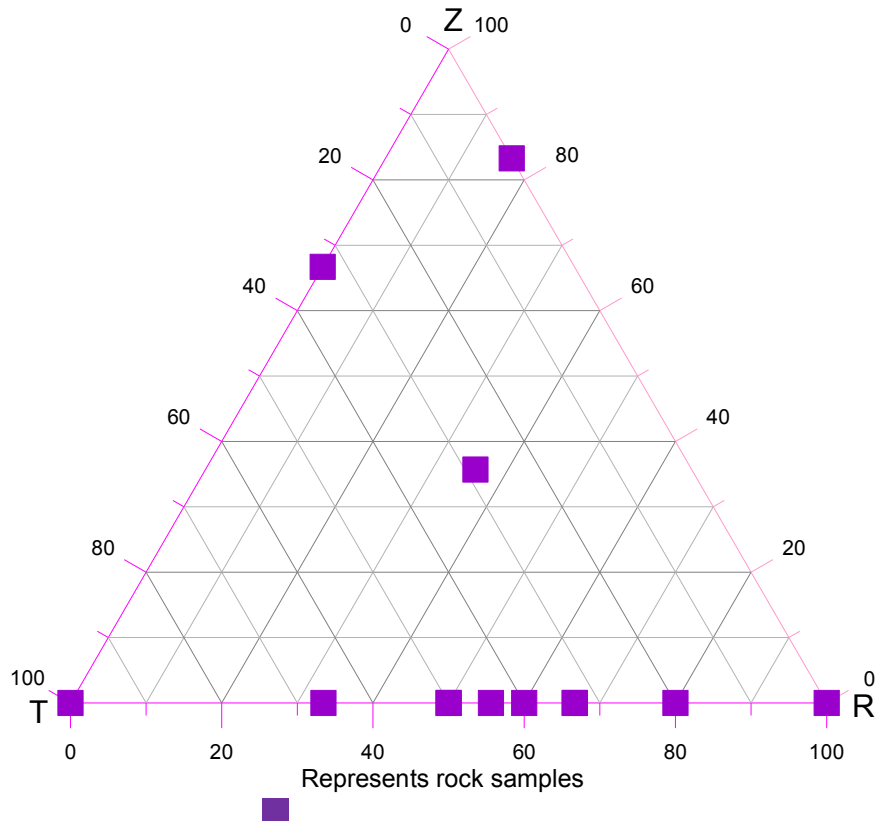


Fig. 10. Ternary plot of ZTR indices for the analysed samples

Table 5. Heavy mineral counts of samples from the studied areas

| Sample no | Z | T | R | E | C | Ti | St | Si | G | Opaque | Non-opaque | ZTR | ZTR index(%) |
|---------------------|----------|----------|----------|----------|----------|-----------|-----------|-----------|----------|---------------|-------------------|------------|---------------------|
| B1 AJALI SANDSTONE | 4 | 2 | - | 16 | 27 | 17 | - | - | - | 108 | 50 | 6 | 12 |
| B2 AJALI SANDSTONE | - | 6 | 6 | 8 | 24 | 5 | - | - | - | 90 | 45 | 12 | 26.6 |
| B3 AJALI SANDSTONE | - | 2 | 3 | 7 | 19 | 4 | 3 | 2 | - | 77 | 37 | 5 | 13.5 |
| B4 AJALI SANDSTONE | 5 | - | 1 | 15 | 22 | 13 | - | - | - | 67 | 52 | 6 | 11.54 |
| B5 AJALI SANDSTONE | - | 6 | 2 | 9 | 24 | 12 | - | - | 5 | 97 | 41 | 8 | 19.5 |
| B6 AJALI SANDSTONE | - | 4 | 5 | 10 | 23 | 5 | - | - | 2 | 83 | 30 | 9 | 30 |
| B7 AJALI SANDSTONE | - | 4 | 4 | - | 16 | - | - | - | - | 23 | 20 | 8 | 40 |
| B8 AJALI SANDSTONE | - | 3 | 6 | 7 | 21 | 4 | - | - | - | 49 | 35 | 9 | 25.7 |
| B 9 AJALI SANDSTONE | - | - | 9 | 4 | 15 | 5 | 2 | - | - | 98 | 54 | 9 | 16.7 |
| B10AJALI SANDSTONE | - | 4 | 8 | 2 | 25 | 4 | - | - | - | 92 | 59 | 12 | 20.3 |
| B11NKPOROMUDSTONE | - | 2 | 8 | 7 | 19 | 6 | - | - | - | 97 | 44 | 10 | 22.72 |
| B12NKPOROSILTSTONE | - | 7 | - | 2 | 15 | 2 | - | - | - | 61 | 21 | 7 | 33.3 |
| B13 MAMU SILTSTONE | 5 | 4 | 5 | 6 | 31 | 20 | - | - | - | 37 | 24 | 14 | 58.3 |

Table 6. Heavy mineral association and their provenance

| Sample no | Mineral association | Provenance |
|----------------------|---|--|
| B1 AJALI SANDSTONE | Tourmaline, Zircon, Epidote, Titanite, Chloritoid. | Acid igneous rock and Dynamothermalmetarmorphic rock |
| B2 AJALI SANDSTONE | Tourmaline, Rutile, Epidote, Titanite, Chloritoid. | Acid igneous rock and Dynamothermalmetarmorphic rock |
| B3 AJALI SANDSTONE | Tourmaline, Rutile, Epidote, Titanite, Chloritoid, Sillimanite, Staurolite. | Acid igneous rock and Dynamothermalmetarmorphic rock |
| B4 AJALI SANDSTONE | Zircon, Epidote, Titanite, Chloritoid, Staurolite. | Dynamothermalmetarmorphic rock |
| B5 AJALI SANDSTONE | Tourmaline, Rutile, Epidote, Titanite, Chloritoid, Garnet. | Acid igneous rock and Dynamothermalmetarmorphic rock |
| B AJALI SANDSTONE 6 | Tourmaline, Rutile, Epidote, Titanite, Chloritoid, Garnet, Zircon. | Acid igneous rock and Dynamothermalmetarmorphic rock |
| B7 AJALI SANDSTONE | Tourmaline, Rutile, Chloritoid. | Acid igneous rock |
| B8 AJALI SANDSTONE | Tourmaline, Rutile, Epidote, Titanite, Chloritoid. | Acid igneous rock and Dynamothermalmetarmorphic rock |
| B9 AJALI SANDSTONE | Rutile, Epidote, Titanite, Chloritoid, Staurolite, Garnet. | Dynamothermalmetarmorphic rock |
| B10 AJALI SANDSTONE | Tourmaline, Rutile, Epidote, Titanite, Chloritoid. | Acid igneous rock and Dynamothermalmetarmorphic rock |
| B11 NKPORO MUDSTONE | Tourmaline, Rutile, Epidote, Titanite, Chloritoid. | Acid igneous rock and Dynamothermalmetarmorphic rock |
| B12 NKPORO SILTSTONE | Tourmaline, Epidote, Titanite, Chloritoid. | Dynamothermalmetarmorphic rock |
| B13 MAMU SILTSTONE | Tourmaline, Rutile, Epidote, Titanite, Chloritoid, Zircon. | Acid igneous rock and Dynamothermalmetarmorphic rock |

The sandstone was also plotted on a QFR ternary plot (Fig. 13) of Dickinson and Suczek [27] for plate tectonic settings, which indicate the settings of the sandstone to be of recycled orogeny provenance. The low relief and long

transport distance gives rise to sub-lithic arenite. The sandstone was also plotted on the QFR ternary plot (Fig. 14) of Suttner et al. [28] to deduce the climatic setting at the time of deposition.

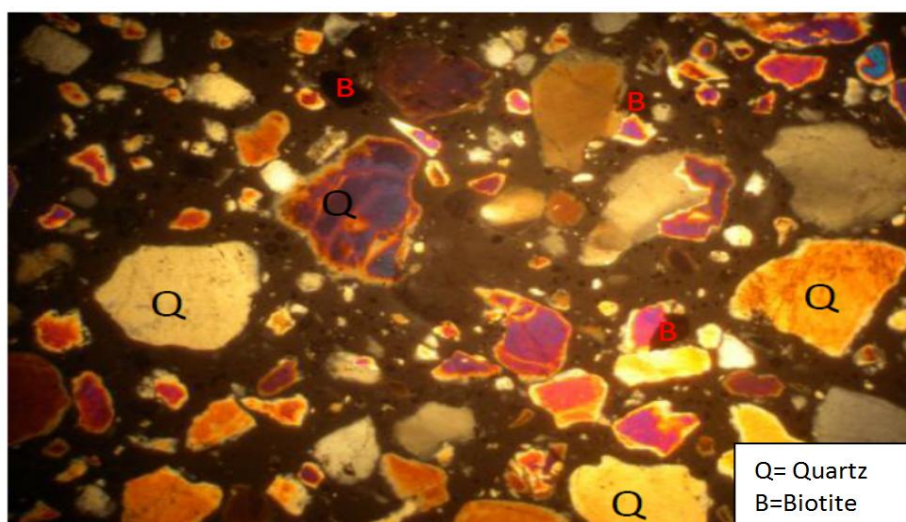


Fig. 11. Photomicrograph of Ajali sandstone sample

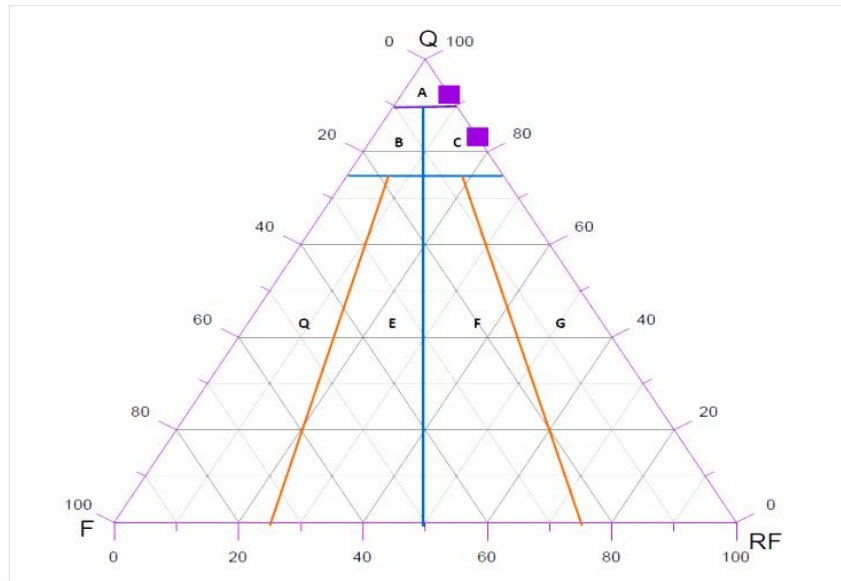


Fig. 12. Ternary classification of sandstone based on framework components after Folk [18]
 A=QUARTZ ARENITE, B=SUBARKOSE, C=SUBLITHARENITE, D=ARKOSE, E=LITHIC ARKOSE,
 F=FELDSPATHIC LITHARENITE, G=LITHARENITE

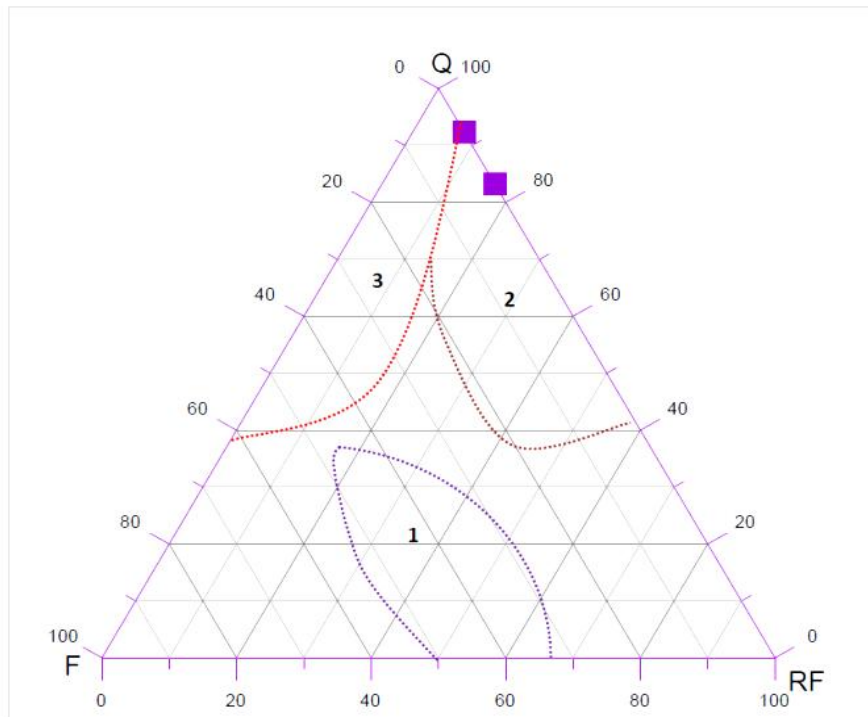


Fig. 13. Palaeotectonic setting of the analyzed samples after Dickinson and Suczek [27]
 1=MAGMATIC ARC PROVENANCE, 2=RECYCLED OROGEN PROVENANCE, 3=CONTINENTAL BLOCK
 PROVENANCE

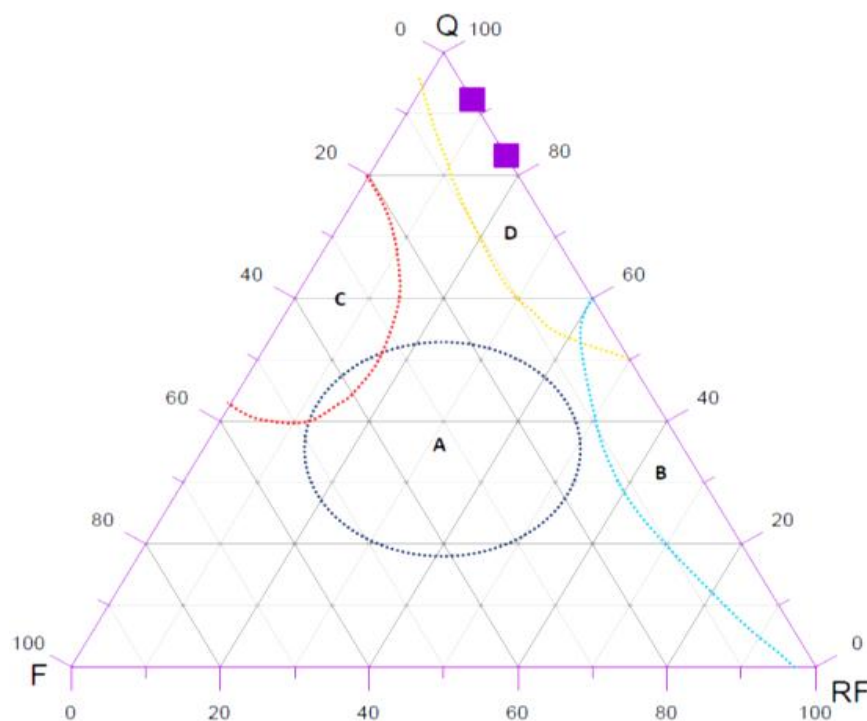


Fig. 14. Palaeoclimatic Setting of the Sandstones after Sutter et.al. [28]
 A=PLUTONIC ARID, B=METAMORPHIC ARID, C=PLUTONIC HUMID, D=METAMORPHIC HUMID

3.11 Palynology Analysis

The nine palynological slides were subjected to microscopic analysis. The samples range from T1–T9 (Table 3) with T1-T3 collected from Nkporo Group, T4-T7 collected from Enugu Formation and T8-T9 collected from Mamu Formation. Generally, the samples (T1-T9) are shales which are fairly moderately rich in palynomorphs while algae show exceedingly high frequency of in some of them. In term of fossil preservation, the forms are corroded (poorly preserved) which show evidence of reworking or insitu weathering of the samples. The samples were collected from different locations, thus, they were treated on individual basis.

Table 7. Recalculated percentage of Ajali sandstone mineral composition

| Sample no | Quartz | Feldspar | Rock fragment |
|-----------|--------|----------|---------------|
| A | 92.3 | 0 | 7.7 |
| B | 83.3 | 0 | 16.7 |

3.11.1 Location T1

This location contains moderate recovery of miospores and algae. Forms that are stratigraphically important present include *Retidiporites magdalenensis*, *Auriculiidites reticulatus*, *Longapertites marginatus*, and *Monocolpites marginatus* (Fig.7) in relatively moderate amount. These forms have been used by earlier workers to establish Maastrichtian sedimentary deposits [29,30]

3.11.2 Location T2

This sample has little recovery of palynomorphs; though, it contains important fossils that are capable of suggesting geologic age of the sediment. Some of the forms contained in the sample are *Retidiporites magdalenensis*, *Proteacidites* sp., *Milfordia* sp., *Zlavisporites blanensis*, *Echitriletes mulleri*, *Monocolpites marginatus* and *Monosulcites* sp. Other forms present are *Tricolpites* sp., *Laevigatosporites* sp., and *Inaperturopollenites* sp. Most of the forms present are suggestive of Maastrichtian age, but an

Early Maastrichtian age is inferred based on the co-occurrence of *Milfordiasp*, *Proteacidite ssp*, *Retidiporites magdalenensis* and *Monocolpitesmarginatus*. Paleoenvironment of deposition is probably transitional environment.

3.11.3 Location T3

This sample is very rich in miospores. The palynomorph abundance and diversity is relatively high and contains quite important marker fossils. Stratigraphically important forms present are *Zlivisporitesblanensis*, *Foveotriletesmargaritae*, *Monocolpitesmarginatus*, *Periretisyncolpitesp*, *Longapertitesmarginatus*, *Cupanieiditesreticulatus*, *Verrucosisporitesp*, *Lycopodiumsp*, *Trioritesp*, *Syncolporitesmarginatus*, *Monocolpopollenitesphaeroidites*, *Echitriporitestrianguliformis*, and *Constructipollenitesineffectus*, (Fig 15). Most of the pollen and spores recovered have been used by earlier workers to date sedimentary deposits of Early Maastrichtian age [31,32,33,34]. The sediment is suggested to have been deposited in a marginal marine environment based on the co-occurrence of Microforaminiferal wall linings, *Phelodiniumbolonienae*, and *Botryococcusbraunii* [30,35].

3.11.4 Location T4

The palynomorph assemblage in the sample is moderate except *Botryococcusbraunii* with very high frequency of recovery. Key fossils present in the sediment include *Constructipollenitesineffectus*, *Monosulcitesp*, *Stephanocolpitesp*, *Longapertitesmarginatus* and *Monocolpitesmarginatus*. (Fig 16) The association of *Stephanocolpitesp* with other miospores present might suggest a Late Maastrichtian deposit [29]. However, the sample is conveniently dated Maastrichtian age. The paleoenvironment of deposition is marginal marine based on the occurrence of *Phelodiniumbolonienae*, Microforaminiferal wall lining and high abundance of *Botryococcusbraunii*. Such phenomenon was reported by [32,30]

3.11.5 Location T5

This sample contains moderate amount of miospores recovery. However, marker forms present are *Cingulatisporitesornatus*,

Longapertitesmarginatus, *Milfordiasp*, *Retidiporites magdalenensis*, and *Monosulcites sp*. Other forms present are *Retitricolpitesp*, *Laevigatosporitesp* and *Inaperturopollenites sp*. The deposit is dated Early Maastrichtian age based on the co-occurrence of *Milfordiasp*, *Cingulatisporitesornatus*, *Retidiporites magdalenensis* and *Longapertitesmarginatus*. *Milfordiasp* is known not have ranged beyond Early Maastrichtian [30]. The environment of deposition is suggested to be marginal marine on the basis of co-occurrence of Microforaminiferal wall linings and strong influence of fresh water form like *Botryococcusbraunii* [30].

3.11.6 Location T6

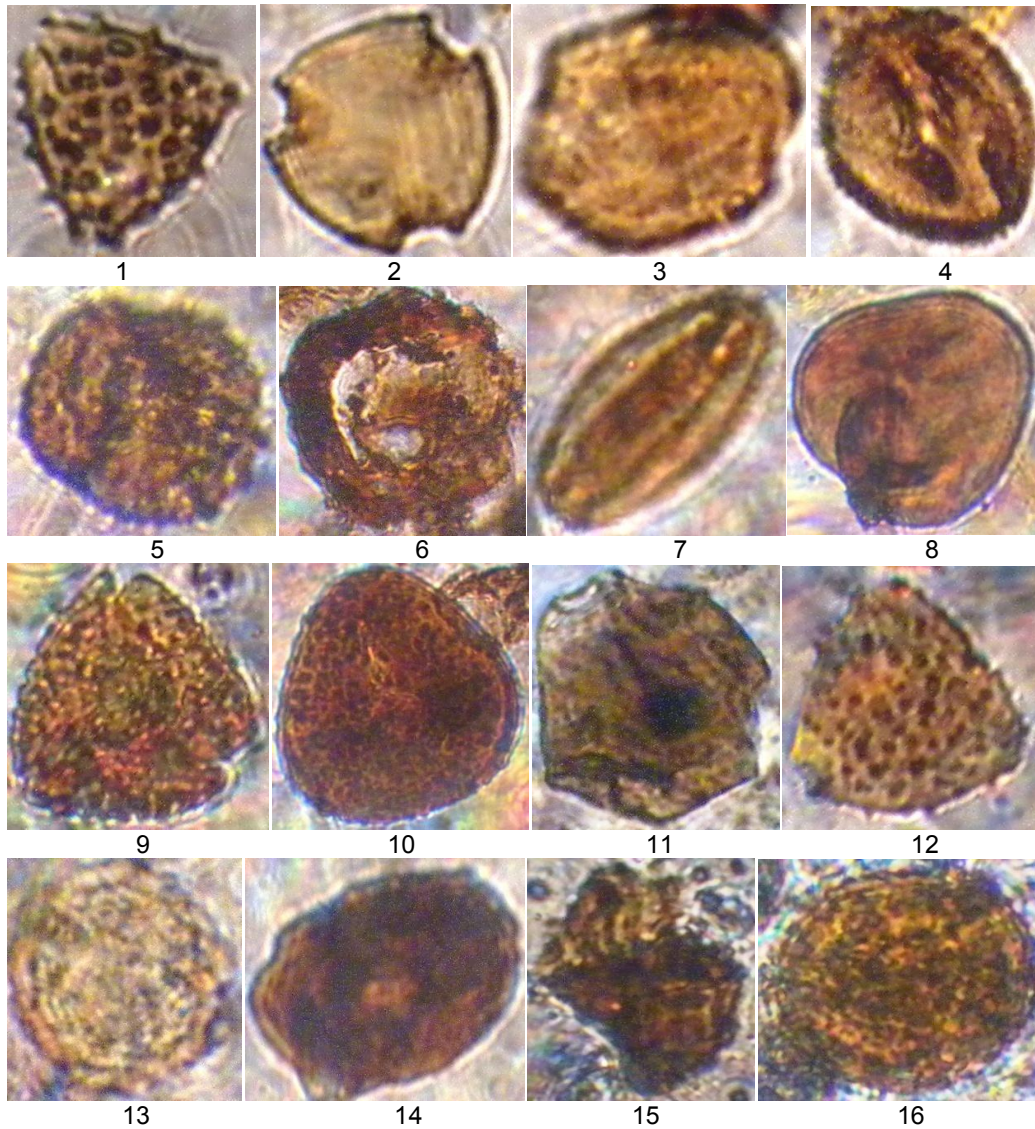
This sample exhibits the same palynomorph assemblage as described for location T5. However, additional marker forms present are *Rugulatisporitesp* and *Dinogymniumundulosum* which further establishes an Early Maastrichtian age for the sediment. *Dinogymniumundulosum* was used to date part of Nkporo Shale exposures on the Calabar Flank, SE Nigeria as Early Maastrichtian [32]. The paleoenvironment of deposition is also marginal marine as described for Location T5.

3.11.7 Locations T7-T9

The Locations T7-T9 is marked by the occurrence of *Longapertitesmicrofoveolatus*, *Longapertitesmarginatus*, *Graminidite ssp*, *Proxapertitescursus*, *Monocolpopollenitesphaeroidites*, *Monocolpitesmarginatus* and *Milfordia sp*. Other miospores present are *Constructipollenitesineffectus*, *Retidiporitesmagadalenensis*, *Syncolporitesp*, *Ephedripitesp*, *Auriculiiditesp*, *Dinogymniumundulosum*, *Monocolpites marginatus*, *Periretisyncolpitesp*, *Verrucosisporitesp*, *Rugulatisporitescuperatus*, *Monosulcitesp*, *Tricolporopollenite ssp* and *Inaperturopollenites sp*.

These assemblages are suggestive of Early Maastrichtian age and similar to reported works [31,32,33,36,29,30]. The paleoenvironment of deposition is suggested to be marginal marine based on the co-occurrence of *Dinogymniumundulosum*, *Senegaliniumsp*, *Phelodiniumbolonienae*, Fungal spore, Microforaminiferal wall linings, and *Botryococcusbraunii* (Fig.15) [35,37,30]

Magnification at ×400



- 1,12 Echitriporitestrianguliformis **Van Hoeken Klinkenberg[34]**
- 2 Tricolpitesp
- 3 Retidiporites magdalenensis **Van der Hammen and Garcia[38]**
- 4 Tricolpopollenitesp
- 5 Tricolpitesp
- 6 Milfordiasp
- 7 Tricolpitesp
- 8 Foveotriletesmargaritae **Germeraad et al[39]**
- 9 Tricolpitesp
- 10 Verrucosisporitesp
- 11 Tricolpitesp
- 13 Stephanocolpitesp
- 14 Milfordiasp
- 15 Dinogymniumundulosum
- 16 Monocolpopollenitesphaeroidites **Jarddine and Magloire[36]**

Fig. 15. Palynomorph A

Magnification at ×400

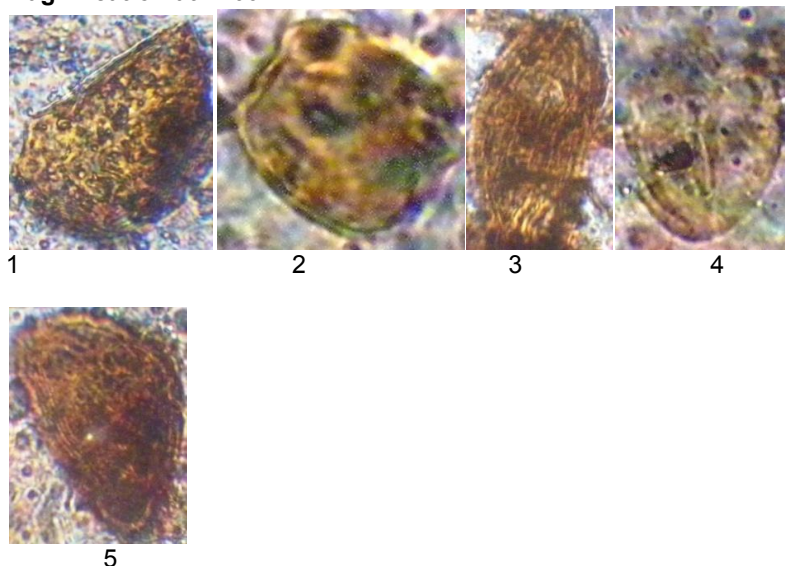


Fig. 16. Palynomorphs B

1. LongapertitesmarginatusVan HoekenKlinkenberg [34]
2. Retidiporites magdalenensisVan der Hammen and Garcia [38]
3. Ephedripitesp
4. MonocolpitesmarginatusVan der Hammen [38]

3.12 Foraminiferal Result

The samples range from T1 – T9 with T1-T4 collected from Enugu Formation, T5-T7 collected from Nkporo Group and T8-T9 collected from Mamu Formation.

Paleoenvironment: Marginal Marine

The dominance of arenaceousforaminiferal species suggest deposition of this sample under Marginal Marine condition.

3.12.1 Sample T1

Species Name: Arenaceous indeterminate
 Species Count: 1
 Age: Indeterminate
 Diagnostic Criteria: Undiagnostic
 Biostratigraphy: *Arenaceous indeterminate*
 Paleoenvironment: Marginal Marine

3.12.2 Sample T2

Species Name: Arenaceous indeterminate
 Species Count: 1
 Age: Indeterminate
 Diagnostic Criteria: Undiagnostic
 Biostratigraphy: *Arenaceous indeterminate*
 Paleoenvironment: Marginal Marine

3.12.3 Sample T3

Species Name: Barren
 Species Count: 0
 Age: Indeterminate
 Diagnostic Criteria: Indeterminate
 Biostratigraphy: Indeterminate
 Paleoenvironment: Indeterminate

3.12.4 Sample T4

Species Name: Haplophragmoides excavate
 Species Count: 15
 Species Name: Haplophragmoidessp
 Species Count: 1
 Age: Coniacian- Maastrichtian
 Diagnostic Criteria: Occurrence of Haplophragmoides excavate
 Biostratigraphy: Haplophragmoides excavate has been reported from Coniacian- Maastrichtian of North America [40,41] Abundant in the Coniacian part of the Nkalagu Paleoenvironment: Marginal Marine. Bassey[42]

3.12.5 Sample T5

Species Name: Haplophragmoides excavate
 Species Count: 2
 Age: Coniacian- Maastrichtian
 Diagnostic Criteria: Occurrence of Haplophragmoides excavate

Biostratigraphy: Haplophragmoides excavate has been reported from Coniacian- Maastrichtian of North America [40,41]. Abundant in the Coniacian part of the Nkalagu Formation and the whole of Nkporo shale in the Calabar Flank Bassey[42].
Paleoenvironment: Marginal Marine.

3.12.6 Sample T6

Species Name: Ammobaculites subcretaceus
Species Count: 56
Species Name: Haplophragmoides excavate
Species Count: 6
Species Name: Trochammina sp.
Species Count: 2
Species Name: Arenaceous indeterminate
Species Count: 2

Age: Maastrichtian

Diagnostic Criteria: Co-occurrence of Ammobaculites subcretaceus and Haplophragmoides excavate

Biostratigraphy: Ammobaculites subcretaceus is restricted to the lower part of the Nkalagu Formation Nyong and Ramanathan [43] reported this species from the exposed late Albian to Cenomanian strata of the Calabar Flank.

Haplophragmoides excavate has been reported from Coniacian- Maastrichtian of North America [40,41]. Abundant in the Coniacian part of the Nkalagu Formation and the whole of Nkporo shale in the Calabar Flank Paleoenvironment: Marginal Marine. Bassey [42].

The dominance of arenaceous foraminiferal species suggests deposition of this sample under Marginal Marine condition.

3.12.7 Sample T7

Species Name: Barren
Species Count: 0
Age: Indeterminate
Diagnostic Criteria: Indeterminate
Biostratigraphy: Indeterminate
Paleoenvironment: Indeterminate

3.12.8 Sample T8

Species Name: Bathysiphonbrosgei
Species Count: 1
Species Name: Haplophragmoides sp.
Species Count: 1
Species Name: Trochammina sp.
Species Count: 1
Species Name: Arenaceous indeterminate

Species Count: 2

Age: Maastrichtian
Diagnostic Criteria: Occurrence of Bathysiphonbrosgei
Biostratigraphy: Bathysiphonbrosgei: the stratigraphic range of this species is Albian to Maastrichtian [40].
Paleoenvironment: Marginal Marine. The dominance of arenaceous foraminiferal species suggests deposition of this sample under Marginal Marine condition.

3.12.9 Sample T9

Species Name: Trochammina sp.
Species Count: 1
Age: Indeterminate
Diagnostic Criteria: Undiagnostic
Biostratigraphy: Trochammina sp.
Paleoenvironment: Marginal Marine.

4. CONCLUSION

The granulometric result and field data suggest that the Ajali Sandstone are medium to coarse grained, poor to moderately sorted, mesokurtic to leptokurtic, and mostly nearly symmetrical sand bodies, with a paleocurrent which runs in a southwest direction. The log probability plot of the sandstone shows three patterns the suspension, saltation and traction. The fine grained particles were transported in suspension while the medium and coarse grained are transported in saltation and traction respectively. All of the samples were transported in saltation, combined with either suspension or traction. The histograms have a unimodal pattern which implies that the Ajali sandstone was deposited by one depositing medium. The sandstones are texturally immature which means that they have not travelled a long distance before deposition, and they are compositionally mature because of the absence of feldspar which is unstable mineral. The sandstone is quartz arenite to sublitharenite with Quartz of 82-93% showing contribution from igneous and metamorphic origin. The bivariate and multivariate result suggest that most of the sandstone of Ajali Formation are fluvial deposit while few others are a shallow marine deposit. The heavy mineral analysis of these sediments suggests two source terrain, which includes acid igneous rock and dynamothermal metamorphic rocks. The ZTR index ranges from 11.5 to 58.3% inferred that they are moderately mature mineralogically. The QFR plot indicates recycled orogeny provenance and humid climatic setting.

The Palynology and Foraminiferal result suggest that the paleoenvironment of Nkporo Shale, Enugu Shale, and Mamu Shale were Marginal marine environment, based on the occurrence of palynomorphs such as *Phelodinium bolonienae*, Microforaminiferal wall linings, a large number of *Botryococcus braunii*, and dominance of arenaceous foraminiferal species. The age of Enugu/Nkporo Shales were suggested to be Early-Late Maastrichtian, the age of Mamu shales were suggested to be Early Maastrichtian, based on the occurrence of palynomorphs such as *Dinogymnium undulosum*, *Phelodinium bolonienae* and *Botryococcus braunii*. Based on the occurrence of foraminiferal such as *Haplophragmoides excavate*, the age of Enugu shale was suggested to be Coniacian-Maastrichtian.

COMPETING INTERESTS

Authors have declared that no competing interests exist.

REFERENCES

1. Murat RC. Stratigraph and pale geography of lower tertiary, Southern Nigeria, in Dessavagie TPJ, Whiteman (Eds.), Afrigeol. University of Ibadan, Nigeria. 1972;425.
2. Short KC, Stauble AJ. Outline of the Geology of Niger Delta. Am. Ass. Petro. Geol. Bull. 1967;51:661-779.
3. Benkheilil J. Benue trough and benue chain. London. Geol. Mag. 1982;119:155-168.
4. Benkheilil J. The origin and evolution of the cretaceous benue trough, Nigeria. Journal of African Earth Science. 1989;8:251-282.
5. Burke KC, Dessavagie TFJ, Whiteman AJ. Geological history of the valley and its adjacent areas. In Dessavagie TFJ, Whiteman AJ. (eds.) African Geology, University of Ibadan Press. 1972;187-205.
6. Fairhead JD. Mesozoic plate tectonic reconstruction of the central South Atlantic Ocean: The role of the west and central African rift systems. Tectonophysics. 1988;155:181-191.
7. Hoque M, Nwajide CS. Tectono-sedimentological evolution of an elongate intracratonic basin (aulacogen): The case of the Benue Trough of Nigeria. Journal of Mining and Geology. 1984;21:19-26.
8. Olade MA. Evolution of Nigeria's Benue Trough (Aulacogen). A Tectonic Model. Geol. Mag. 1975;112:575-583.
9. Olade MA. Review of Nigerian Pre-cretaceous: In Reyment RA (ed.) aspects of the geology of Nigeria, Ibadan, Univ. Press. 1978;16-22.
10. Petters SW. Stratigraphic evolution of the Benue trough and its implication for the upper Cretaceous paleogeography of West Africa Jour. Geol. 1978;86:311-322.
11. Agagu OK. Geology and petroleum potential of Santonian to Maastrichtian sediments in Anambra Basin, eastern Nigeria. Unpublished PHD Thesis. University of Ibadan; 1978.
12. Obaje NG, Ulu OK, Petters SW. Biostratigraphic and geochemical controls of hydrocarbon prospects in the Benue Trough and the Anambra Basin, Nigeria. NAPE Bull. 1999;14(1):18-54.
13. Reyment RA. Aspect of the Geology of Nigeria. Ibadan University Press. 1965; 145.
14. Simpson A. The Nigerian coal fields, the geology of parts of Onitsha, Owerri and Benue Provinces. Geol Surv. Nigeria. Bull. 1954;24:85.
15. Tatttam CM. A review of Nigeria stratigraphy, Report Geol. Surv of Nigeria. 1944;27-46
16. Adeigbe OC, Salufu AE. Geology and depositional environment of campano-maastrichtian sediments in the Anambra basin, south eastern Nigeria: Evidence from Field Relationship and Sedimentological Study. Earth Sci. Res. J. 2009;13(2):148-166.
17. Steinmetz, R. Analysis of vectorial data. Journal of Sedimentary Research. 1962; 32(4):801-812.
18. Folk RL. Petrology of sedimentary rocks. Texas Hemphil. Pub. Co. 1974;182.
19. Faegri K, Iversen J. Textbook of pollen analysis. Faegri K, Kaland PE, Krzywinski K, editors. New York: John Wiley & Sons. 1989;328.
20. Traverse A. Palaeopalynology Unwin Hyman, London. 1988;1-600.
21. Wood GD, Gabriel AM, Lawson JC. Palynological techniques—processing and microscopy. In: Jansonius J, McGregor V, editors. Palynology: principles and applications. American Association of Stratigraphic Palynologists Foundation, Dallas. 1996;1:29-50.

22. Green OR. A manual of practical laboratory and field techniques in Palaeobiology Kluwer academic publishers, Dordrecht. 2001;538.
23. Folk RL, Ward WC. Brazos River Bar. A study in the significance of grain size parameters. Journal of Sedimentary Petrology. 1957;27:3-26.
24. Sahu R. Textural parameter: An evaluation of fluvial and shallow marine deposits. Journal Sed. Pet. 1964;34:513-520.
25. Friedman GM. Dynamic process and statistical parameters compared for size frequency distribution of beach and river sands. Journal of Sedimentary Petrology. 1967;37(2):327-352.
26. Moiola RJ, Weiser D. Textural parameters and evaluation. Journal of Sedimentary Petrology. 1968;38:45-53.
27. Dickson WR, Suczek CA. Plate tectonics and sandstone composition. AAPG Bull. 1979;63:2164-2182.
28. Suttner LJ, Basu A, Mach GH. Climate and the origin of Quartz-arenites. Journal Sed. Petrology. 1981;51:1235-1246.
29. Lawal O, Moullade M. Palynological biostratigraphy of the Cretaceous sediments in the upper Benue Basin NE. Nigeria. Revue Micropaleontologie. 1986; 29(1):61-83.
30. Ola-Buraimo AO, Adeleye M. Palynological characterization of the late Maastrichtian coal measure deposit, southwestern Nigeria. Science Focus. 2010;15(2):276-287.
31. Adebayo OF, Ojo AO, Ola-Buraimo AO. Upper cretaceous spore-pollen zonation, southern bida basin, Central Nigeria. Jour. of Applied Environ. Scien. 2007;3(2):170-175.
32. Edet JJ, Nyong EE. Palynostratigraphy of Nkporo Shale exposures (Late Campanian-Maastrichtian) on the Calabar Flank, SE Nigeria. Review of Paleobotany and Palynology. 1994;80:131-147.
33. Ikhane PH, Akintola AJ, Ola-Buraimo AO, Oyebolu OO, Akintola GO, Adesanwo BT. Palynology and paleoenvironmental reconstruction of the early maastrichtian afowo formation, dahomey basin, southwestern Nigeria. Science Journal of Environmental Engineering Research. 2011;2:8. ISSN: 2276-7495
34. Van Hoeken-Klinkenberg PMJ. A palynological investigation of some Upper Cretaceous sediments in Nigeria. Pollenet Spores. 1964;6(1):209-231.
35. Schrank E. Organic-walled microfossils and sedimentary facies in the Abu Tartur phosphates (Late Cretaceous, Egypt). Berlin Geowiss, Abh (A). 1984; 50:177-187.
36. Jardine S, Magloire I. Palynologie et stratigraphic du cretace des basins du Senegal et de Cote d' Ivoire ler Coll. Memoire du. Bureau Recherches Geologiques et Minieres. 1965;32:187-245.
37. Ojo OJ, Akande SO. Depositional environments and diagenesis of the carbonate facies of dakul and Jessau formations in the yola Basin NE Nigeria. Implications reservoir potential. Nigeria Association of Petroleum Explorationists Bulletin. 2000;15:47-50.
38. Van der H. Boletin Geologico (Bogota), 1954;2(1):49-106.
39. Germeraad JH, Hopping CA, Muller J. Review paleobotany and palynology. 1968;6:189-348.
40. Martin L. Upper cretaceous and lower tertiary foraminifera from Fresno county, California. Jb. CeoL Bund. Sondb. 1964; 9:1-128.
41. Sliter WV. Upper cretaceous foraminifera from southern California anr J Northwestern Baja California, Mexico. - Univ. Kansas Paleont. Contr. Ser. 49, Protozoa. 1968;7:1-141.
42. Bassey EC. Cretaceous foraminiferal biostratigraphy of the subsurface of the Calabar Flank. Unpublished doctoral dissertation. Dep't of Geology, University of Calabar; 1991.
43. Nyong EE, Ramanathan RM. A record of oxygen deficient paleoenvironments in the Cretaceous of the Calabar flank, Southeast Nigeria. J Afr Earth Sci. 1985;3(4):455-460.

© 2018 Ayorinde et al.; This is an Open Access article distributed under the terms of the Creative Commons Attribution License (<http://creativecommons.org/licenses/by/4.0>), which permits unrestricted use, distribution, and reproduction in any medium, provided the original work is properly cited.

Peer-review history:
 The peer review history for this paper can be accessed here:
<http://www.sciencedomain.org/review-history/24473>